Journal of Engineering and Applied Sciences 15 (2): 468-478, 2020
ISSN: 1816-949X

Assessment of CO_2 Adsorption Capacity under Moderate Pressure Range on Activated Carbon Produced from Coconut Endocarp

[1, 2]Paulo Cardozo Carvalho de Araújo, [3]Degival Rodrigues Gonçalves Júnior,
[4]Antônio Santos Silva, [1]Rodolpho Rodrigues Fonseca, [2]Lucio Cardozo-Filho,
[5]José Jailton Marques, [6]Diógenes R.L. Vedoy and [1]Edilson de Jesus
[1]Department of Chemical Engineering, Quebec Experience Program,
Federal University of Sergipe São Cristóvão, Sergipe, Brazil, South America
[2]Department of Chemical Engineering, State University of Maringá, Maringá, Paraná,
Brazil, South America
[3]Laboratory of Chemical Analysis, Agro-Campolindo Industry, Nossa Senhora das Dores,
Sergipe, Brazil, South America
[4]Department of Mathematics, Quebec Experience Program,
University of Sergipe São Cristóvão, Sergipe, Brazil, South America
[5]Department of Environmental Science and Engineering,
Federal University of Sergipe São Cristóvão, Sergipe, Brazil, South America
[6]Department of Chemical and Materials Engineering, University of Alberta,
Edmonton, Alberta, Canada

Abstract: In this study, we prepared activated carbon using coconut residue (*Cocos nucifera* L.) and evaluate the potential use of this activated carbon for capture and storage of carbon dioxide (CO_2). Regeneration tests indicated that the activated carbon has a good regenerative capacity and maypotentially be used in CO_2 adsorption systems. For example, the ability of the activated carbon to capture and then release CO_2 is not significantly affected even after three consecutive adsorption/desorption cycles, regardless of the temperature tested (either 125, 150 or 180°C). Kinetic studies revealed that the time required for total saturation of the activated carbon was 25 min for the pressure range investigated (0.14-0.34 MPa). This ability to retain considerable amounts of CO_2 quickly under low pressures is likely due to the presence of microporous at the surface of this adsorbent, as suggested by reports in the literature and the morphological features of the activated carbon presented here. In addition, equilibrium studies using the Langmuir and Freundlich isotherms showed that the activated carbon has a maximum adsorption capacity of 76.03 mg g^{-1} at 15°C. This adsorption capacity decreases with temperature increase, reaching 58.84 mg g^{-1} at 35°C. Similar behavior has been observed for other absorbents and is expected for adsorption processes due to the exothermic nature of these processes. In summary, the results indicated that the activated carbon produced with coconut residue has great potential as a CO_2 absorbent.

Key words: Coconut endocarp, CO_2 removal, adsorption, equilibrium, kinetics, temperature

INTRODUCTION

There is worldwide consensus that one of the biggest environmental problems today is the increase in the CO_2 concentration in the Earth's atmosphere, mainly due to the burning of fossil fuels and is reflected in the worsening of the greenhouse effect.

Among the existing techniques to promote a reduction in carbon dioxide emissions, CO_2 Capture and Storage (CCS) technologies are becoming more prominent, since, they are the most effective in the short and medium term to reduce uncontrolled release of carbon dioxide into the atmosphere or to promote the capture of the gas already present in the atmosphere (Xenias and Whitmarsh, 2018).

The CO_2 capture and storage process can be carried out by several techniques but the one that stands most for its efficiency and economic viability is adsorption. Its principle is based on the preferential accommodation of the gas inside the porous at the surface of the adsorbent.

There are some adsorbents that are used for the CO_2 adsorption process (Soleha *et al*., 2019), among them activated carbon stands out for having a large surface area that can be modified by chemical agents (H_3PO, $ZnCl_2$ and KOH) and physical agents which are produced from various precursors. Because of this great advantage, it is possible to obtain a new class of lower-cost alternative charcoal which is synthesized from agroindustrial waste (Gottipati and Mishra, 2013).

Corresponding Author: Marechal Rondon Avenue, Cidade Universitária, José Aloísio Campos, Jardim Rosa Elze,
CEP 49100-000 Telephone/fax: +55-79-21056676/+55-79-21056890

Brazil is also one of the world's largest producers of coconuts (*Cocos nucifera* L.) with about 800 million fruits produced annually. Brazil also discards 5 million tons per year just in the form of endocarp and fibers in the states of Bahia and Sergipe which respectively account for 32.8 and 13.5% of national production (De Souza *et al*., 2012; Rodrigues *et al*., 2018).

However, these residues have been widely applied in several segments, especially in synthesizing activated carbon because of the low production cost. In the pyrolysis process, the coconut endocarp produces a hard and granulated charcoal which has been used in the adsorption of dyes, heavy metals, organic and inorganic compounds and acidic gases such as CO_2 and H_2S (Lin *et al*., 2015).

Inspired by the applications reported above, we attempted to capture CO_2 using activated carbon produced from coconut (*Cocos nucifera* L.) endocarp residue. This work involved the development of a CO_2 capture and storage system. In this case, a fixed bed adsorption process with online acquisition of the system pressure data was used which enabled evaluating the adsorptive capacity and kinetic behavior of CO_2 adsorption by the activated carbon via. the static volumetric method.

MATERIALS AND METHODS

Synthesis of activated carbon: Activated carbon was produced by pyrolyzing coconut endocarp (*Cocos nucifera* L.) impregnated by certain amount of phosphoric acid (85% purity). Prior to pyrolysis, the material was washed with distilled water to remove pulp and fibers, broken into small pieces and then oven dried for 1 h at 105°C. Next, the coconut endocarp mixture with H_3PO_4 in a 1:3 mass ratio [200 g of endocarp to 300 mL of phosphoric acid (600 g)] (Haimour and Emeish, 2006) was heated for 1 h at 80°C under agitation in order to promote greater action by the activating agent on the endocarp surface. Finally, the material was filtered to remove the excess acid and dried in an oven for 24 h at 80°C, followed by oven pyrolysis (Fig. 1) at 700°C for 2 h with a heating ramp of 25°C min^{-1} and a N_2 flow of 1 L min^{-1}. The obtained activated carbon was then washed with distilled water, dried for 24 h at 80°C and stored in a desiccator in order to avoid contact with the environment and humidity.

Morphology: The morphology of the activated carbon was studied before and after the adsorption process using a scanning electron microscope (JCM-5700 Jeol Carry Scope) under the following conditions: nominal resolution of 1000 and 3000 times and a beam acceleration voltage of 5 kV. A N_2 adsorption method proposed by Brunauer, Emmett and Teller (BET) was used to determine the characteristics of the activated carbon's porous structure using a surface area, volume and pore distribution meter (Micromeritics, model ASAP 2020) in the range of 0.0463-0.3469 in terms of relative pressure. Helium gas pycnometry was used to determine the actual specific mass of the activated carbon with the assistance of a

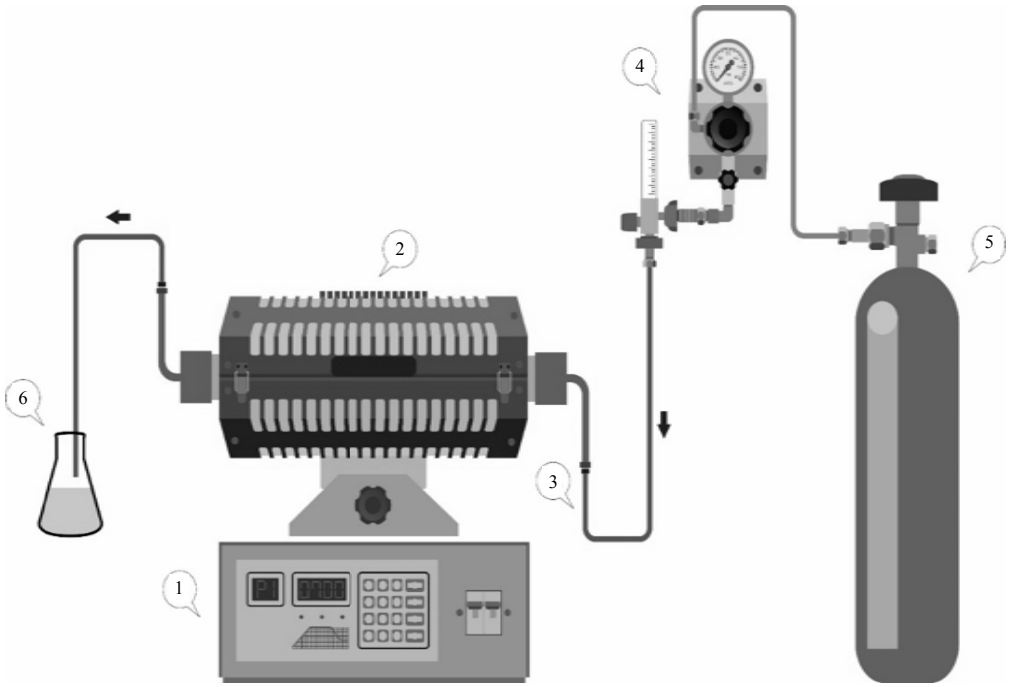

Fig. 1: Scheme of the pyrolysis furnace (1) Furnace power supply with temperature programming, (2) Pyrolysis furnace, (3) Connecting hoses, (4) N2 flow regulating valve and pressure gauge, (5) Cylinder containing N2 and (6) Pyrolysis gas neutralization container

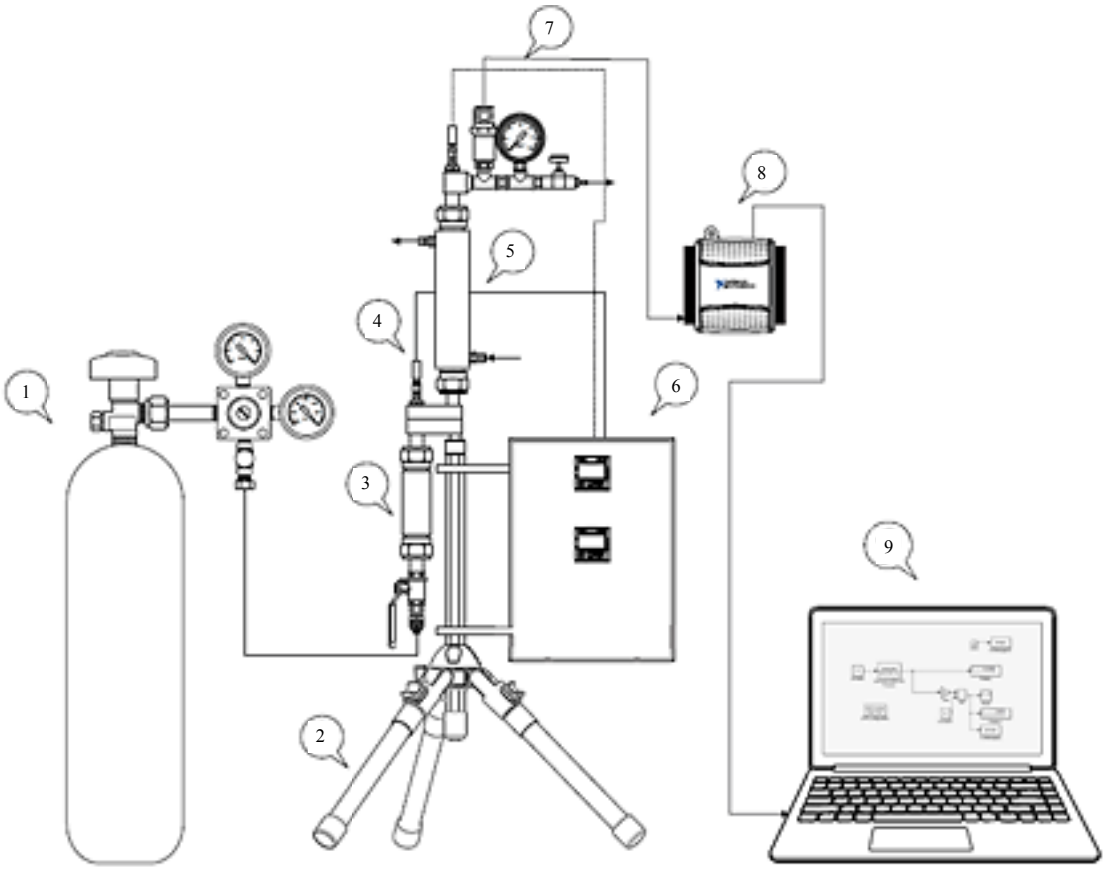

Fig. 2: Fixed bed adsorption system with online pressure data acquisition

Helium pycnometer (Micromeritics, model AccuPyc II 1340). Finally, a thermobalance (Shimadzu, model DTG-60H) was used to evaluate the mass loss of the synthesized carbon due to possible chemical and physical transformations as a function of temperature (TG/DTG and DTA). The experiment was performed under nitrogen flow in a pre-established temperature range of 297.15-1173.15 K with a heating ramp of 10 K min^{-1}.

Fixed bed adsorption system: The adsorption assays were performed in a fixed bed adsorption system designed with online pressure acquisition, according to Fig. 2. The supervisory system consisted of a work area created in Matlab/SIMULINK® Software (9) integrated with an acquisition board (National Instruments, model USB-6008) (8) for acquiring the column pressure variation signals picked up by the pressure transmitter (Velki, model VKP-011) with a measuring capacity of 0-2 MPa (7). The adsorption column (5) was made of stainless steel (ANSI 304) with 20 mm of internal diameter and 25 cm of height with a thermal jacket with inlet and outlet in 1/4" NPT spigot connections, allowing the establishment of temperature during adsorption by means of an ultra thermostatic bath (Quimis, model Q2114M2). The lower part of the column contains a gas reservoir (3), provided with a 1/4" NPT needle valve at the end to control the CO_2 input (99% White Martins) from a cylinder (4). At the upper ends of the reservoir and column (4) two temperature sensors (Ecil, PT-100 type) were connected to two temperature controllers (NOVUS, model N1030) (6) which enabled monitoring the temperature during the adsorption tests.

Kinetics and equilibrium models: The equilibrium and kinetic data for the CO_2 adsorption process were obtained using the static volumetric method proposed by Sarker *et al*. (2017) which required the use of a pressurized fixed bed column (Fig. 2) containing 2 g of activated carbon (#4-9-Tyler scale). The activated carbon was previously dried in an oven for 1 h at 110°C in contact with an initial amount of CO_2 determined from the initial pressures of 0.14, 0.18, 0.22, 0.26, 0.30 and 0.34 MPa in the temperatures of 15, 24 and 35°C, thereby enabling an evaluation of the dynamics of the system's initial pressure drop until the equilibrium pressure. The adsorption capacity was calculated by the ratio of the adsorbed gas mass to the used adsorbent mass.

The kinetic models consideredin this study included a pseudo-first-order model, Eq. 1 and pseudo-second-order model, Eq. 2 (Alvarez-Gutierrez *et al*., 2017). The kinetic models were adapted to the experimentally measured variable (pressure) via. a data acquisition board:

$$\frac{dP_t}{dt} = K_1(P_e - P_t) \quad (1)$$

$$\frac{dP_t}{dt} = K_2(P_e - P_t)^2 \quad (2)$$

where, P_e and P_t (mg g^{-1}) are the measured pressures of the adsorption system at equilibrium and at time "t", respectively, K_1 (sec^{-1}) is the first-order adsorption rate constant and K_2 (MPa^{-1} sec^{-1}) is the kinetic constant of the pseudo-second-order

The adsorption equilibrium data are usually obtained by means of isotherms which consist of linear or non-linear relations at constant temperature between the adsorbed amount of CO_2 and the equilibrium system pressure. The Langmuir and Freundlich models are presented as one of the most used adsorption isotherms to describe experimental data on the equilibrium of CO_2 adsorption systems in activated carbon and zeolites (Chou *et al*., 2013).

The Langmuir isotherm, Eq. 3, takes into account that the adsorption occurs in a monolayer on a surface with a defined number of sites, adopting the premise that the adsorbate surface is energetically homogeneous:

$$q_e = \frac{q_{max} b P_e}{1 + bP_e} \quad (3)$$

where, q_e (mg g^{-1}) is equilibrium adsorption capacity at a given pressure, q_{max} (mg g^{-1}) is maximum amount of CO_2 adsorbed and b (Mpa^{-1}) are the Langmuir Model parameters and P_e is the equilibrium pressure of the adsorption system].

The Freundlich isotherm, Eq. 4, assumes that the adsorption occurs in multilayers, being convenient to describe an adsorptive process on a heterogeneous surface (Saghafi and Arabloo, 2017):

$$q_e = K_F P_e^{\,n} \quad (4)$$

where, K_F [(mg g^{-1}) $(Mpa)^{-n}$] is the constant of the Freundlich Model and n the parameter that is related to the energy heterogeneity of the adsorbent surface.

In the experimental routines, the equilibrium pressure (P_e) was determined by reading the system pressure at the equilibrium point and the amount of CO_2 adsorbed by the activated carbon (q_e) is inferred through the relation between the number of free CO_2 mol at the beginning of the process and in equilibrium by the mass of adsorbent used. The volume occupied by the free CO_2 inside the column was calculated by Eq. 5:

$$V_d = V_t - V_s \quad (5)$$

Considering V_d is the volume occupied by CO_2 in the column, V_t is the total volume of the system (138.5 cm^3) and V_s is the volume occupied by the adsorbent.

The volume occupied by the adsorbent was established by means of Eq. 6:

$$V_s = \frac{m}{\rho} \quad (6)$$

Where:
V_s : The volume occupied by the activated carbon
m : The mass of the activated carbon
ρ : The density of the activated carbon

In calculating the number of mol at the beginning of the process and in equilibrium, we used Eq. 7 and 8, respectively:

$$n_{initial} = \frac{V_d}{(V_m)_{inicial}} \quad (7)$$

$$n_{eq} = \frac{V_d}{(V_m)_{eq}} \quad (8)$$

Where:
$n_{initial}$: The number of mol of CO_2 at the beginning of the process
n_{eq} : The number of mol of CO_2at equilibrium
V_d : The volume occupied by the CO_2 in the column
$(V_m)_{initial}$: The specific volume of CO_2 at the beginning of the process
$(V_m)_{eq}$: The specific volume of CO_2 at equilibrium

The specific volume of CO_2 at the beginning of the process and at equilibrium were determined by the truncated virial state equation in the second term with Pitzer correlations for calculating the second virial coefficient (B) due to the low pressures used in the adsorption process in this research (0.1-0.5 MPa) (Smith *et al*., 2007). These correlations are presented by means of Eq. 9-13:

$$B^0 = 0.083 - \frac{0.422}{T_r^{1,6}} \quad (9)$$

$$B^1 = 0.139 - \frac{0.172}{T_r^{4,2}} \quad (10)$$

$$B = \frac{RT_c}{P_c}(B^0 + \omega B^1) \quad (11)$$

$$Z = 1 + \frac{BP}{RT} \quad (12)$$

$$V_m = \frac{ZRT}{P} \quad (13)$$

Where:
T_r : The reduced temperature
T_c : The critical temperature
R : The universal constant of gases
P_c : The critical pressure
P : The initial pressure or at equilibrium
ω : The acentric factor for CO_2
Z : The compressibility factor
V_m : The specific volume of the initial CO_2 or at equilibrium

The variation in the number of mol of CO_2, provided by Eq. 7 and 8 in turn established the actual amount of CO_2 that was adsorbed by the activated carbon which enabled obtaining the mass of CO_2 adsorbed through the ratio of the number of mol by the molar mass of the carbon dioxide (44.1 g mol^{-1}) with the maximum amount of CO_2 adsorption by the activated carbon being determined by Eq. 14:

$$q_e = \frac{m_{CO_2}}{m} \quad (14)$$

Where:
q_e : The equilibrium adsorption capacity
m_{CO2} : The mass of adsorbed CO_2
m_{ads} : The mass of the adsorbent

The parameters of the kinetic and equilibrium models were estimated using the least squares method using the objective function according to Eq. 15:

$$F_{obj} = \sum_{i=1}^{NE} (q_e^{calc} - q_e^{meas})^2 \quad (15)$$

Where:
NE : The number of experiments
q_e^{meas} : The dependent variable being measured experimentally
q_e^{calc} : The dependent variable obtained by the mathematical model

Regeneration cycles: The regenerative capacity of activated carbon was evaluated by means of three adsorption/desorption cycles. The experiments were carried out in batch in which about 2 g of activated carbon impregnated with CO_2 were regenerated by heating in an oven (Sterilifer, model SX 1.0) at temperatures of 125, 150 and 180°C for 1 h. The regenerated carbon was reused for CO_2 adsorption by establishing the initial pressure of 0.3 MPa at a temperature of 24°C, repeating the process three times for each regeneration temperature. The CO_2 removal percentage was calculated using Eq. 16:

$$\text{Removal (\%)} = \frac{(P_i - P_e)}{P_i} \times 100 \quad (16)$$

In which P_i and P_e, respectively represent the initial and equilibrium pressure of the adsorption system.

RESULTS AND DISCUSSION

Morphology of the activated carbon: Figure 3a and b show that the activated carbon surface consists of hexagonal and heterogeneous structures with about 10 μm pores which have cavities, cracks and particles of various sizes inserted into the pores. Figure 3c and d indicate the presence of CO_2 inside the pores, resulting in a different morphology for the activated carbon after CO_2 adsorption.

Table 1 presents values that describe the textural characteristics of the activated carbon surface. These values were obtained according to the BET method.

The pore diameter value found herein indicates that the activated carbon surface has microporous according to the IUPAC classification (0-2 nm). In addition, the surface morphology observed in this study was similar to the one reported by Hauchhum and Mahanta (2014) (214 m^2 g^{-1} of surface area) who also used coconut endocarpas precursor for the production of activated carbon.

Studies presented by Calvo-Munoz *et al*. (2016) showed that different materials synthesized from biomass residues have great CO_2 adsorption potential when these materials are used in their post-combustion conditions, room temperature and pressure of 0.10 MPa. The researchers also reported that pores with diameters lower than 0.8 nm are the ones directly responsible for the ability of these materials to retain CO_2 at lower pressure ranges (<0.4 MPa).

The density found in this study (1.6305 g cm^{-3}) was similar to the onefound in the study by Guerra *et al*. (1.6740 g cm^{-3}) who used the same raw material (the coconut endocarp)as in this research to produce a granular activated carbon.

Furthermore, before the CO_2 adsorption (Fig. 4a), the TG/DTG curves showed a mass decrease in the range of 100-200°C, associated to the loss of 0.10 g/g of moisture, with a characteristic band on the DTA curve of one phase change. There was a gentle slope in the TG curve between 250-500°C, associated to the slow degradation of organic compounds of the activated carbon. Another considerable point of mass loss (about 0.12 g/g) in the range of 700-850°C can be associated with the decomposition reactions of some inorganic components present in the activated carbon. This observation is consistent with the descending DTA curve in this temperature range and typical of endothermic process reactions. Similar observation was reported by Radic *et al*. (2017).

Table 1: Textural characteristics of the produced activated carbon

Properties	Activated carbon
Surface area (m^2 g^{-1})	268.32
Pore volume (cm^3 g^{-1})	0.116
Pore diameter (nm)	0.183

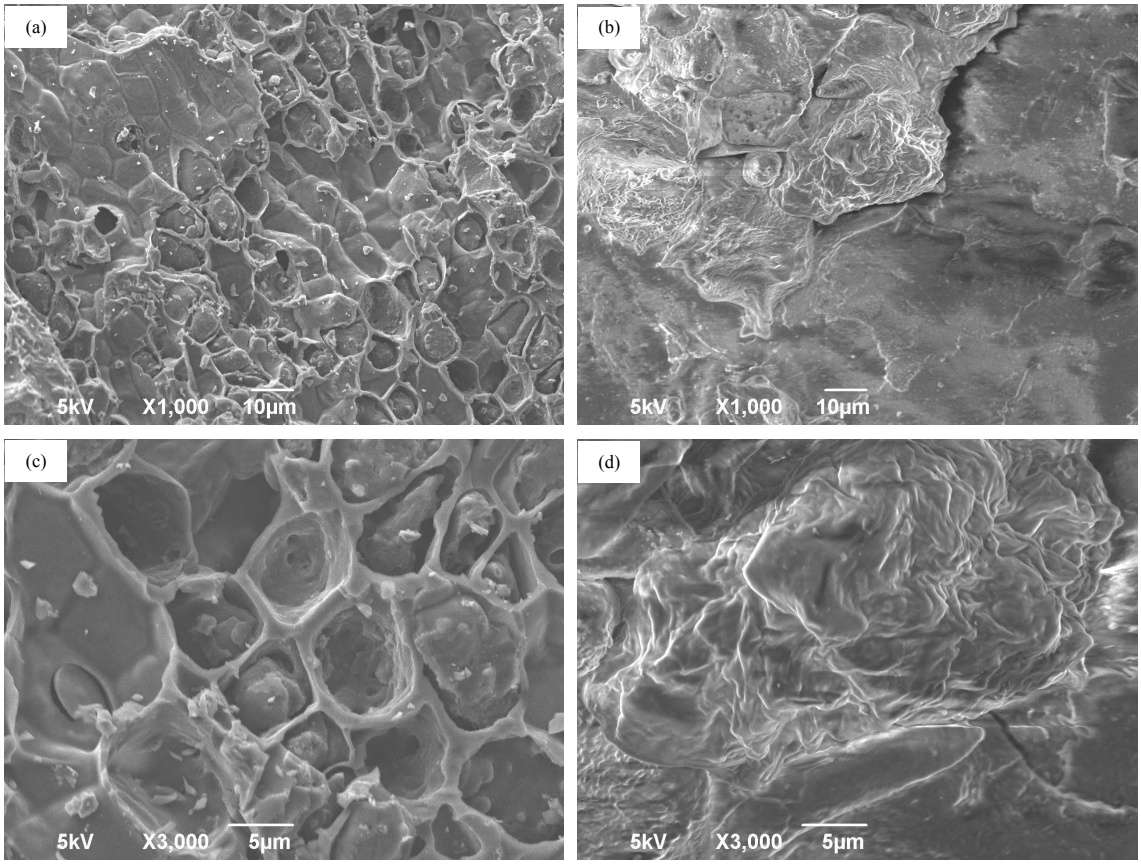

Fig. 3(a-d): Micrographic images of the produced activated carbon (a) Before the CO_2 adsorption at 1000x, 3000x and (b) After the CO_2 adsorption at 1000x and 3000x

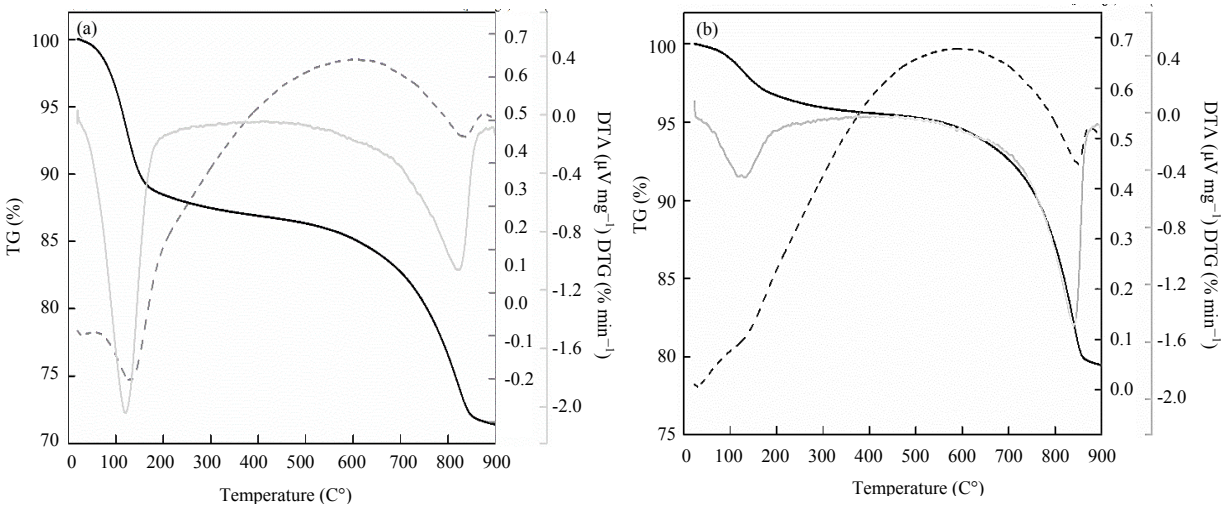

Fig. 4(a-b): Thermal analysis of the produced activated carbon: (a) Before adsorption and (b) After CO_2 adsorption

After the CO_2 adsorption process (Fig. 4b), a lower mass loss variation was observed in the 100-200°C temperature range in the TG/DTG curves. This lower variation is due to the drying of the activated carbon

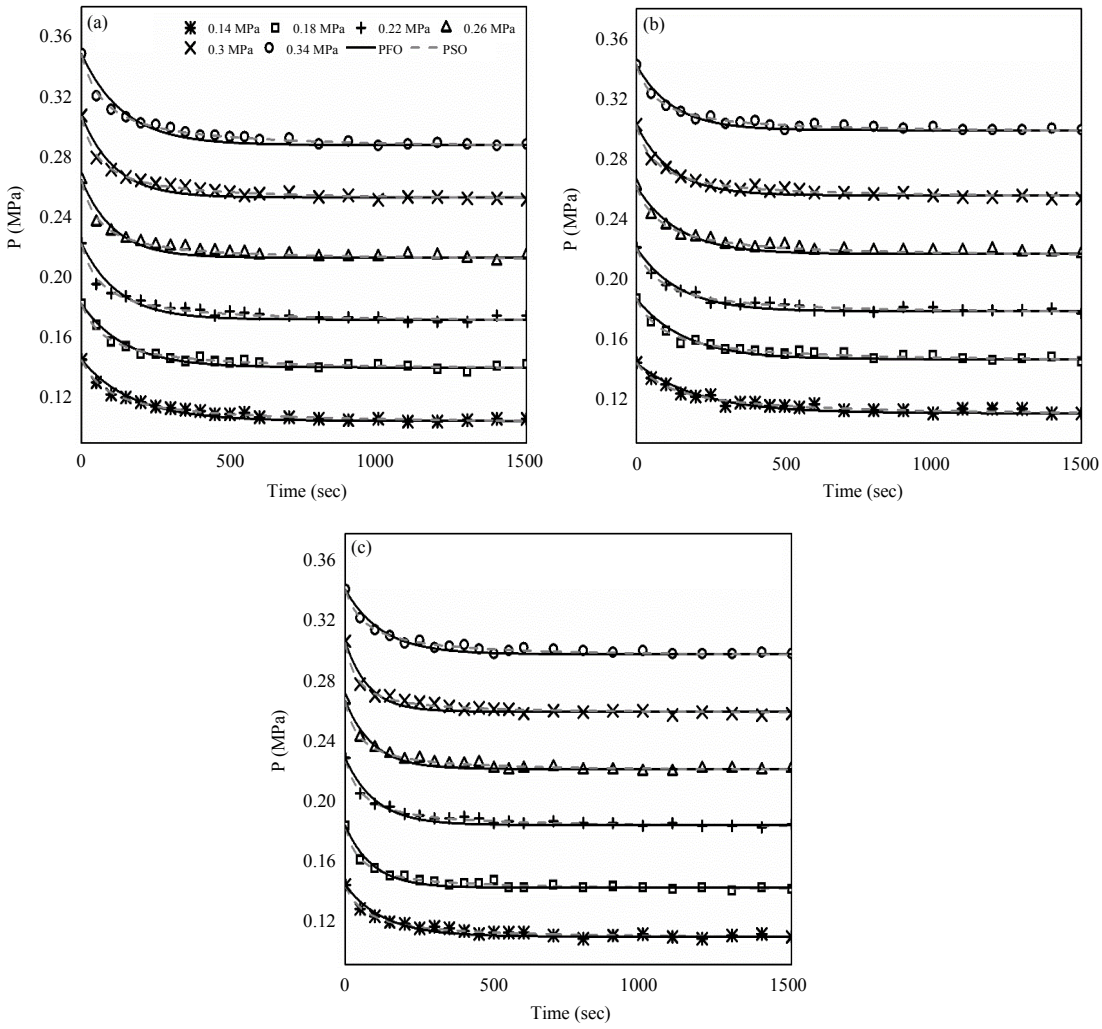

Fig. 5(a-c): CO_2 adsorption kinetics on activated carbon at different temperatures, (a) 15°C, (b) 24°C and (c) 35°C

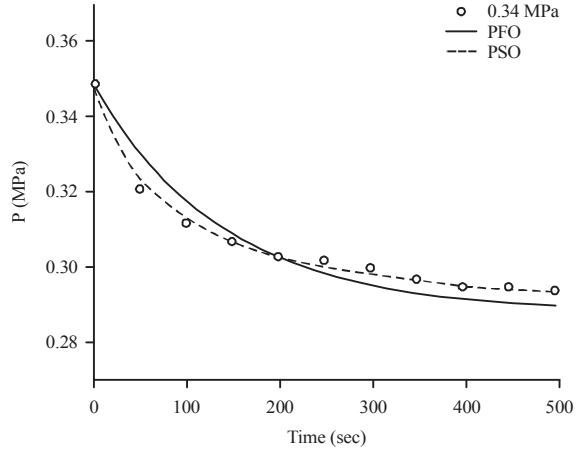

Fig. 6: Kinetic curve at the condition of 15°C and initial pressure of 0.34 Mpa

before the adsorption process. On the other hand, the higher slope for the TG/DTG curve band in the 700-850°C temperature range can again be associated with the decomposition reactions of inorganic compounds which have probably interacted with CO_2, corresponding to the largest descending band on the DTA curve.

Adsorption kinetics: The kinetics of CO_2 adsorption at the surface of activated carbon were evaluated under initial system pressure ranging between 0.14-0.34 MPa and at temperatures of 15, 24 and 35°C. The results (kinetic curves in Fig. 5) showed that adsorption occurs rapidly during the first few minutes of the process and reaches equilibrium in approximately 1500 sec, thus, presenting great similarity to the saturation time reported by Shafeeyan *et al*. (2015) (1200 sec).

The pseudo-second-order model was the best fit for the experimental data, according to Fig. 6. The parameters of the pseudo-first and pseudo-second-order kinetic

Table 2: Pseudo-first-order kinetic model parameters at 15, 24 and 35°C

		Pseudo-first-order				
Temperature (°C)	Pi (MPa)	K_1 (sec^{-1})	Error in k_1 (10^{-5})	P_e (MPa)	Error in P_e (10^{-4})	R^2
15	0.14	0.0058	13.605	0.1046	0.1450	0.9492
	0.18	0.0068	16.985	0.1402	0.1450	0.9468
	0.22	0.0081	36.380	0.1720	0.2850	0.9171
	0.26	0.0091	38.135	0.2131	0.2250	0.9241
	0.30	0.0089	30.780	0.2531	0.2250	0.9401
	0.34	0.0071	28.055	0.2879	0.3250	0.9406
24	0.14	0.0048	14.345	0.1098	0.1650	0.9246
	0.18	0.0061	18.705	0.1458	0.1850	0.9325
	0.22	0.0071	19.255	0.1778	0.1600	0.9416
	0.26	0.0071	26.960	0.2161	0.2350	0.9232
	0.30	0.0084	23.070	0.2552	0.1650	0.9455
	0.34	0.0081	29.785	0.2988	0.2050	0.9221
	0.14	0.0076	17.585	0.1087	0.1050	0.9381
35	0.18	0.0108	31.850	0.1416	0.1350	0.9337
	0.22	0.0098	33.385	0.1838	0.1740	0.9288
	0.26	0.0107	24.950	0.2215	0.1150	0.9517
	0.30	0.0128	44.750	0.2602	0.1650	0.9305
	0.34	0.0081	29.785	0.2988	0.2050	0.9221

Table 3: Pseudo-second-order kinetic model parameters at 15, 24 and 35°C

		Pseudo-second-order				
Temperature (°C)	Pi (MPa)	K_2 (MPa sec^{-1})	Error in k_1 (10^{-5})	P_e (MPa)	Error in P_e (10^{-5})	R^2
15	0.14	0.0234	31.400	0.1021	0.6500	0.9810
	0.18	0.0262	52.650	0.1377	0.9500	0.9732
	0.22	0.0281	51.400	0.1695	0.9000	0.9777
	0.26	0.0308	37.450	0.2106	0.6000	0.9854
	0.30	0.0290	24.000	0.2505	0.4500	0.9906
	0.34	0.0200	18.450	0.2846	0.6000	0.9907
24	0.14	0.0208	56.950	0.1072	0.1250	0.9578
	0.18	0.0238	32.500	0.1432	0.6500	0.9806
	0.22	0.0275	57.300	0.1754	0.9500	0.9717
	0.26	0.0247	40.500	0.2134	0.8500	0.9786
	0.30	0.0311	47.700	0.2529	0.7000	0.9804
	0.34	0.0306	78.500	0.2964	0.1150	0.9653
	0.14	0.0385	61.300	0.1070	0.6000	0.9725
35	0.18	0.0472	91.150	0.1399	0.7000	0.9724
	0.22	0.0382	67.000	0.1817	0.7500	0.9764
	0.26	0.0439	72.700	0.2197	0.6500	0.9786
	0.30	0.0523	10.085	0.2585	0.7000	0.9759
	0.34	0.0306	78.500	0.2964	0.1150	0.9653

models with their respective errors are presented in Table 2 and 3. The adsorption rate constants of the second-order model increased proportionally to the temperature in the adsorption bed, indicating that the adsorption rate is higher at lower temperatures (where these constants are smaller). Shafeeyan *et al*. (2015) also observed similar decrease on adsorption rates with increasing temperature. This behavior is due to the exothermic nature of the adsorption of CO_2 at the surface of activated carbon.

Adsorption isotherms: Figure 7 shows CO_2 adsorption equilibrium isotherms for three different temperatures (15, 24 and 35°C) and initial system pressure between 0.14 and 0.34 MPa.

The results indicated that the activated carbon was able to capture rapidly considerable amounts of CO_2 under small to moderate initial pressures (0.14-0.34 MPa). Similar behavior was reported in the work of Ogungbenro *et al*. (2017) and Calvo-Munoz *et al*. (2016).The Langmuir and Freundlich models described well the experimental data (Table 4) since, the Langmuir and Freundlich parameters were significant for all the experimental conditions tested as demonstrated by the small error in the Langmuir and Freundlich parameters obtained using a 95% confidence interval.

Also, the adsorption capacities in the pressure range of 0.14-0.34 MPa were 53.90-76.03 mg g^{-1} at 15°C, 43.01-62.37 mg g^{-1} at 24°C and 43.01-58.84 mg g^{-1} at

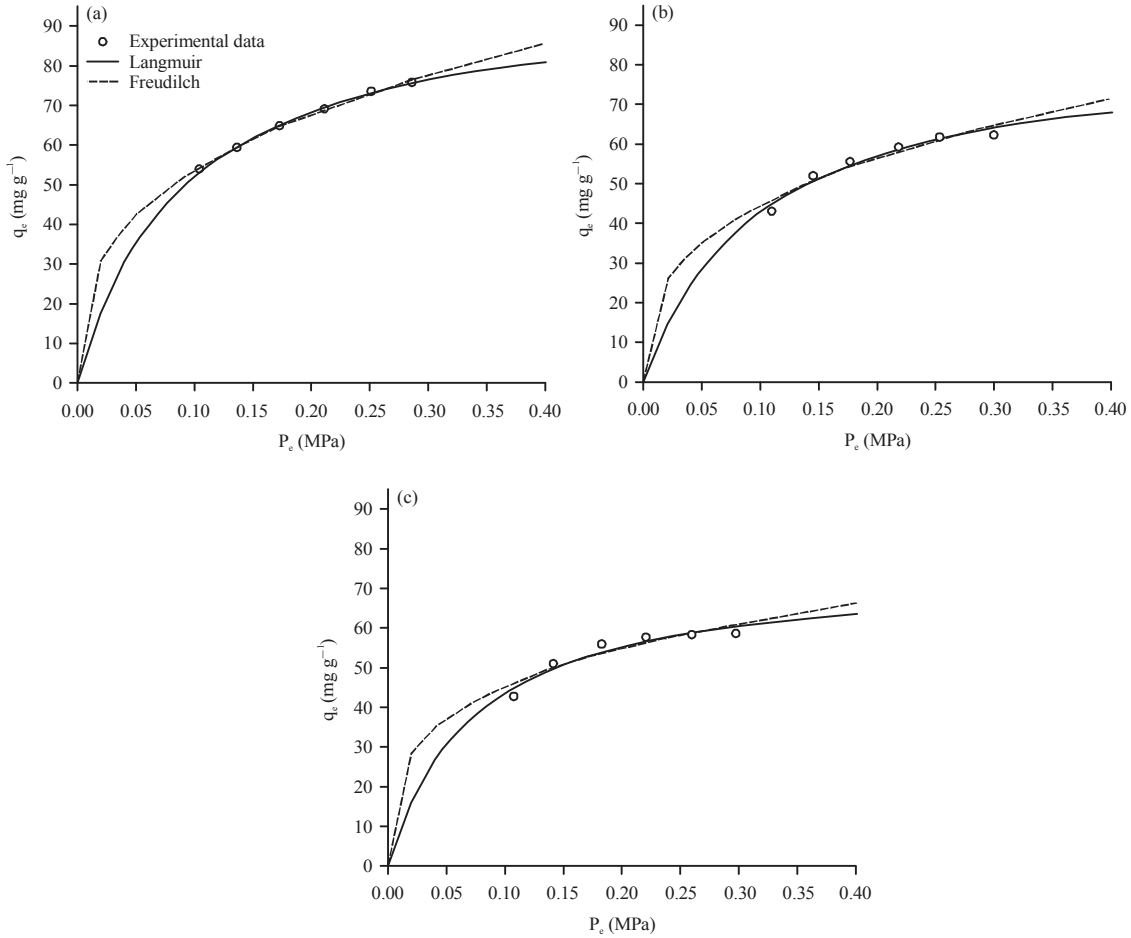

Fig. 7(a-c): CO_2 adsorption equilibrium isotherms at different temperatures (a) 15°C, (b) 24°C and (c) 35°C

Table 4: Parameters of the Langmuir and Freundlich isotherms for the temperatures of 15, 24 and 35°C

	Langmuir			Freundlich		
Temperature (°C)	qmax (mg g^{-1})	b (MPa^{-1})	R^2	K_F [(mg g^{-1}) (MPa)$^{-n}$]	n	R^2
15	99.3964±1.8261	11.1522±0.0682	0.9980	116.9536±1.4991	0.3383±0.0077	0.9991
24	84.5995±4.8521	10.3921±1.7990	0.9827	97.6141±9.43184	0.3405±0.0502	0.9615
35	75.1995±4.9436	14.1028±3.4167	0.9582	85.7224±8.6030	0.2770±0.0615	0.9245

35°C. These results are very similar to the ones found by Singh and Kumar (2016) and in agreement with the typical effect of pressure and temperature on the capacity of activated carbon to absorb CO_2 reported in the literature: increasing the initial system pressure leads to greater CO_2 adsorption by the activated carbon whereas increasing temperature typically reduces the ability of the absorbent to retain CO_2.

In fact, Hauchhum and Mahanta (2014) attributed this inverse relationship between temperature and CO_2 adsorption capacity to the exothermic nature of the adsorption process, as evidenced by the negative enthalpy values of adsorption found by these researchers. In addition, the researchers observed an increase in the internal energy of the adsorbate with temperature increase which makes the local diffusion mechanisms more difficult, facilitating the release of CO_2 molecules from the activated carbon surface.

Regeneration cycles: To evaluate the regenerative capacity of the activated carbon, this material was submitted to three consecutive adsorption/desorption cycles at constant temperatures of 125, 150 and 180°C.

The removal of CO_2 increased after each regeneration cycle for all temperatures tested (Fig. 8a) with the highest removal percentage being at 180°C. In the same way, the adsorbed amounts of CO_2 also increased progressively after each regeneration cycle (Fig. 8b) even after three consecutive adsorption/desorption cycles, indicating that the activated carbon prepared with coconut residue has a goodregenerative capacity and can be used in CO_2 adsorption systems.

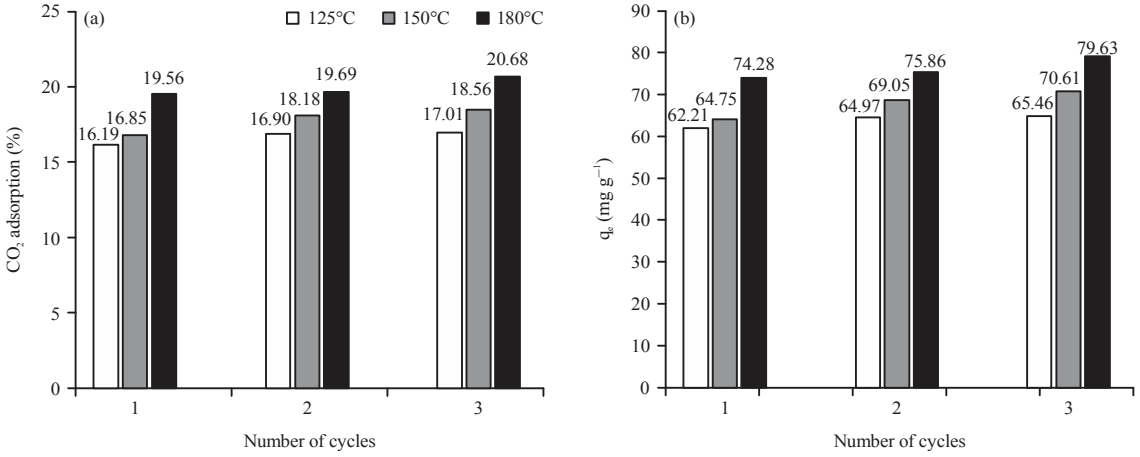

Fig. 8: Regeneration cycles of the produced activated carbon (a) Removal percentage and (b) Amounts adsorbed

CONCLUSION

This study demonstrated that the activated carbon prepared from coconut residue is a great adsorbent for CO_2 and may be used incapture and storage systems for CO_2. For example, regeneration tests showed that the ability of activated carbon to retain CO_2 is not significantly affected even after 3 cycles of adsorption/desorption at 3 different temperatures (125, 150 and 180°C).

In addition, adsorption tests showed that the activated carbon prepared in this study has great capacity to adsorb CO_2 at low pressures due to the presence of microporous at the surface of the adsorbent. In fact, the CO_2 adsorption occurs rapidly in the first minutes of the process with total saturation of the activated carbon occurring around 1500 sec as demonstrated by the kinetic study presented here.

In the same way, the effect of temperature on the adsorption process was also evaluated with the assistance of the Langmuir and Freundlich models. The results revealed that the adsorption capacity of the activated carbon decreased with temperature increase. For example, when the highest initial system pressure is used (0.34 MPa), CO_2 capture by the activated carbon decreases from 76.03 mg g^{-1} at 15°C to 62.37 mg g^{-1} at 24°C and then to 58.84 mg g^{-1} at 35°C. This behavior is expected since adsorption processes are exothermic in nature.

Overall, the activated carbon produced from coconut residue showed great potential to be used as an adsorbent for CO_2 capture and storage.

ACKNOWLEDGEMENT

The researchers give thanks to CAPES (Coordenação de Aperfeiçoamento de Pessoal de Nível Superior), FAPITEC-SE and the Universida de Federal de Sergipe for the financial support.

REFERENCES

Alvarez-Gutierrez, N., M.V. Gil, F. Rubiera and C. Pevida, 2017. Kinetics of CO_2 adsorption on cherry stone-based carbons in CO_2/CH_4 separations. Chem. Eng. J., 307: 249-257.

Calvo-Munoz, E.M., F.J. Garcia-Mateos, J.M. Rosas, J. Rodriguez-Mirasol and T. Cordero, 2016. Biomass waste carbon materials as adsorbents for CO_2 capture under post-combustion conditions. Front. Mater., 3: 1-14.

Chou, C.T. and F.H. Chen, Y. Huang and H.S. Yang, 2013. Carbon dioxide capture and hydrogen purification from synthesis gas by pressure swing adsorption. Chem. Eng., 32: 1855-1860.

De Souza, I.V., M.G. Gondim, A.L.R. Ramos, E.A. dos Santos and M.I. Ferraz *et al*., 2012. Population dynamics of *Aceria guerreronis* (Acari: Eriophyidae) and other mites associated with coconut fruits in Una, state of Bahia, Northeastern Brazil. Exp. Appl. Acarol., 58: 221-233.

Gottipati, R. and S. Mishra, 2013. Preparation of microporous activated carbon from *Aegle marmelos* fruit shell by KOH activation. Canadian J. Chem. Eng., 91: 1215-1222.

Haimour, N.M. and S. Emeish, 2006. Utilization of date stones for production of activated carbon using phosphoric acid. Waste Manage., 26: 651-660.

Hauchhum, L. and P. Mahanta, 2014. Kinetic, thermodynamic and regeneration studies for CO_2 adsorption onto activated carbon. Intl. J. Adv. Mech. Eng., 4: 27-32.

Lin, X.W., Z.B. Xie, J.Y. Zheng, Q. Liu and Q.C. Bei *et al*., 2015. Effects of biochar application on greenhouse gas emissions, carbon sequestration and crop growth in coastal saline soil. Eur. J. Soil Sci., 66: 329-338.

Ogungbenro, A.E., D.V. Quang, K. Al-Ali and M.R.M. Abu-Zahra, 2017. Activated Carbon from date seeds for CO_2 capture applications. Energy Procedia, 114: 2313-2321.

Radic, D.B., M.M. Stanojevic, M.O. Obradovic and A.M. Jovovic, 2017. Thermal analysis of physical and chemical changes occuring during regeneration of activated carbon. Therm. Sci., 21: 1067-1081.

Rodrigues, G.S., C.R. Martins and I. de Barros, 2018. Sustainability assessment of ecological intensification practices in coconut production. Agric. Syst., 165: 71-84.

Saghafi, H. and M. Arabloo, 2017. Estimation of carbon dioxide equilibrium adsorption isotherms using Adaptive Neuro Fuzzy Inference Systems (ANFIS) and regression models. Environ. Prog. Sustainable Energy, 36: 1374-1382.

Sarker, A.I. and A. Aroonwilas and A. Veawab, 2017. Equilibrium and kinetic behaviour of CO_2 adsorption onto zeolites, carbon molecular sieve and activated carbons. Energy Procedia, 114: 2450-2459.

Shafeeyan, M.S., W.M.A.W. Daud, A. Shamiri and N. Aghamohammadi, 2015. Modeling of carbon dioxide adsorption onto ammonia-modified activated carbon: Kinetic analysis and breakthrough behavior. Energy Fuels, 29: 6565-6577.

Singh, V.K. and E.A. Kumar, 2016. Comparative studies on CO_2 adsorption kinetics by solid adsorbents. Energy Procedia, 90: 316-325.

Smith, J.M., H.C.V. Ness and M.M. Abbott, 2007. Introduction to Chemical Engineering Thermodynamics. 7th Edn., McGraw-Hill Education Labs, Boston, Massachusetts, USA.

Soleha, M.Y., O.K. Khim, W.M.Z.W. Yunus, J.I.A. Rashid and A. Fitrianto *et al*., 2019. Thermally treated alum sludge as novel adsorbent of carbon dioxide (CO_2). J. Eng. Appl. Sci., 14: 405-414.

Xenias, D. and L. Whitmarsh, 2018. Carbon Capture and Storage (CCS) experts attitudes to and experience with public engagement. Intl. J. Greenhouse Gas Control, 78: 103-116.